An Evaluation Platform for Catheter Ablation Navigation

An Evaluation Platform for Catheter Ablation Navigation

Florian Heemeyer, Christophe Chautems, Quentin Boehler, José L. Merino and Bradley J. Nelson

Abstract— **Cardiac arrhythmia refers to a condition of an abnormal or irregular heartbeat, which usually results in disturbed blood flow. This can lead to a reduced cardiac output and an increased risk for blood clot formation, which can cause life-threatening heart failure or stroke. Radio-frequency catheter ablation is becoming the treatment of choice for most cardiac arrhythmias. To recover the normal heartbeat, the abnormal excitation sites inside the heart are first identified and then isolated or destroyed by applying radio-frequency energy through the use of an ablation catheter. The design and precise navigation of these ablation catheters is currently a topic of considerable interest. However, the lack of a standardized evaluation setup for catheter ablation makes it challenging to properly compare different systems. In this paper, we present an evaluation platform to tackle this problem. The setup consists of a 3D printed anatomical model, a tracking system for the catheter and a dedicated graphical user interface. The performance of a catheter ablation system can then be assessed based on various performance metrics, such as the procedure duration, contact stability or the ablation angle. Finally, we conduct a proof-of-concept study to demonstrate the usefulness of the proposed setup.**

I. INTRODUCTION

In 2016, approximately 46.3 million people suffered from atrial fibrillation worldwide [1]. This number is estimated to at least double in the coming decades due to an aging population [2]–[4]. Atrial fibrillation is the most common type of cardiac arrhythmia and is associated with irregular contraction of the atria. The resulting decrease of blood flow promotes blood clot formation leading to a significantly increased risk for stroke. As as result, atrial fibrillation accounts for 20-30% of all strokes [5], [6].

The sources causing atrial fibrillation are so-called triggers in the heart (usually located in the pulmonary veins) that rapidly fire and, thereby, disturb the normal heartbeat [7]. While anti-arrhythmic drugs are often the first-line therapy to restore and maintain the natural sinus rhythm, they are associated with a significant atrial fibrillation recurrence rate (63% after 1 year) [7]. Furthermore, anti-arrhythmic drugs are linked with severe adverse effects such as liver, lung and thyroid toxicity. Radio-frequency (RF) catheter ablation is a minimally-invasive alternative treatment showing a reduced atrial fibrillation recurrence rate of ca. 13% after 1 year [7]. In RF ablation, an ablation catheter is advanced through the femoral vein of the patient to the affected region in the heart. When the catheter reaches the desired location, an electrode at the distal tip of the catheter generates RF energy and, thereby, damages the affected tissue directly or electrically isolates the triggers by ablating the surrounding tissue. Many factors influence the overall procedure outcome. In particular, the quality of the ablations mainly depends on the applied power, pulse duration, contact stability, ablation angle and contact force [8]–[10].

The scientific community has made a considerable effort to move from manual catheters to robotic navigation systems as more precise catheter manipulation leads to more reproducible and predictable ablation results. Furthermore, robotic systems show fast learning curves and, thereby, allow less experienced surgeons to perform this highly complex procedure [11]. This is an important benefit considering the shortage of surgeons and the projected rise in atrial fibrillation cases. Currently, there are two main companies offering commercial robotic systems for catheter ablation: Hansen Medical Inc. (Mountain View, CA, USA) and Stereotaxis Inc. (St. Louis, MO, USA). Hansen Medical focuses on an electro-mechanical pull-wire system in which the user operates a master console mirroring his movements through a slave catheter. Stereotaxis develops remote magnetic navigation systems in which they apply external magnetic fields to a magnetic catheter for steering [12].

Despite the effort in developing novel robotic systems for catheter ablation, the studies to assess the performance of these systems are mainly of a qualitative and subjective nature. Steven et al. showed in an in-vivo study that robotic navigation systems decreased RF duration and concluded that improved catheter stability was responsible for this decrease [13]. Pappone et al. came to a similar conclusion and additionally reported easy backtracking to previous targets using remote magnetic navigation [14]. Several other studies presented initial qualitative observations with robotic navigation systems or general success rates [15]–[17]. Additionally, Boehler et al. and Bhaskaran et al. presented in-vitro setups to assess the performance of robotic ablation systems in which they assessed single performance indicators in an isolated manner [10], [18].

Improved catheter navigation will play a crucial role in making ablation procedures more reproducible and predictable. Hence, we introduce a platform that allows for a fair comparison between different catheter navigation approaches. In particular, our contributions are an easy-to-set-up platform for simulated pulmonary vein isolation and Key Performance Indicators (KPIs) for a meaningful comparison between different navigation approaches. Furthermore, surgeons can use the platform to familiarize themselves with

Florian Heemeyer, Christophe Chautems, Quentin Boehler and Bradley J. Nelson are with the Institute of Robotics and Intelligent Systems, ETH Zurich, Tannenstrasse 3, Zurich CH-8092, Switzerland (e-mail: fheemeyer@ethz.ch; christophe.chautems@wysszurich.ch; qboehler@ethz.ch; bnelson@ethz.ch).

José L. Merino is with the Arrhythmia and Robotic Electrophysiology Unit, University Hospital La Paz, Paseo de la Castellana 261, 28046 Madrid, Spain (e-mail: jlmerino@arritmias.net).

the navigation and manipulation properties of new systems.

Our evaluation platform is presented in Sec. II. We first introduce the physical setup as well as the tracking system that we use to localize the ablation catheter. We then present a dedicated graphical user interface (GUI) for progress tracking and visualization of the procedure within an anatomical model of the heart. We also introduce KPIs to evaluate catheter navigation. To demonstrate the usefulness of our setup, we compare and evaluate the performance of two different navigation approaches in a proof-of-concept study in Sec III. In particular, we compare a manual catheter navigation to a remote magnetic navigation approach. Finally, we discuss the usefulness as well as the shortcomings of the presented setup and give an outlook to our future efforts in this field in Sec. IV.

II. MATERIALS AND METHODS

A. Anatomical Model

Atrial fibrillation refers to a condition of chaotic atrial contraction. This is often triggered by electrical sources in the myocardial sleeves, which are muscle sleeves at the base of the pulmonary veins [19]. The electrical isolation of these triggers from the rest of the left atrium is a common way to recover and maintain the normal heartbeat [7]. This procedure is called pulmonary vein isolation. In pulmonary vein isolation, a catheter is inserted into the femoral vein of the patient and advanced to the right atrium. From there, the left atrium is accessed through a puncture in the atrial septum. After successfully accessing the left atrium, the operator can navigate the ablation catheter to the pulmonary veins and ablate tissue around them to properly isolate the triggers. We designed a heart phantom from a public dataset, as shown in Fig. 1 (A), to simulate a pulmonary vein isolation procedure. The user must perform realistic navigation movements with the ablation catheter in order to reach the intended ablation targets in the anatomical model. At the beginning of each experiment, an insertion sheath is advanced through the model so that the distal end is located in the left atrium as shown in Fig. 1 (A). Subsequently, the ablation catheter is pushed through the insertion sheath such that the catheter tip also reaches the left atrium. Two endoscopic cameras track the catheter throughout the procedure to provide information about the catheter tip position and orientation.

Our heart phantom consists of two individual parts that are shown in Figs. 1 (B) and (C). The main part, shown in Fig. 1 (B), holds the two endoscopic cameras as well as the anatomy in which the catheter is inserted and supported. The ablation section, shown in Fig. 1 (C), contains the pulmonary veins and can be attached to the main part to complete the anatomy of the left atrium. We designed the ablation section to be detachable from the main part to allow for the calibration of the stereo camera setup. We will further elaborate the calibration and tracking process in Sec. II-B. We 3D printed the described model using the rigid VeroWhite material (Stratasys Ltd., Eden Prairie, MN, USA) and the Connex350 3D printer (Stratasys Ltd., Eden Prairie, MN, USA) to have a physical setup in which the catheter can be navigated.

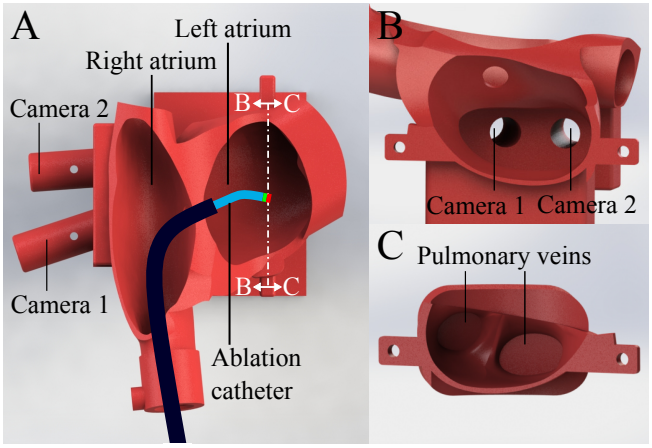

Fig. 1. Heart phantom for the in-vitro pulmonary vein isolation. (A) The ablation catheter is advanced from the femoral vein to the right atrium and into the left atrium through a transseptal puncture. (B) The main part of the setup has a mount for two endoscopic cameras. This stereo camera setup is calibrated and then used to track the 3D pose of the catheter tip. (C) The triggers causing atrial fibrillation often lie in the pulmonary veins. In pulmonary vein isolation, the operator ablates points around these veins to electrically isolate the triggers and restore the normal heartbeat.

Furthermore, a digital copy of the model was created. We use this digital copy to visualize the real-time catheter position and orientation inside the anatomical model in our GUI. Additionally, the GUI allows the user to upload or manually define an ablation trajectory. The trajectory is represented by equally-spaced ablation targets around the pulmonary veins, which are displayed in the GUI along with the catheter tip and the anatomical model. Similar to a real catheter ablation procedure, the user can now navigate the catheter in a physical setup and receive visual feedback through a GUI. The collected navigation data can then be used to quantify the navigation performance.

B. Tracking

The localization of the ablation catheter plays a crucial role in our experimental setup: it provides visual feedback to the user for steering the catheter and allows the user to quantify the performance of the experiment.

While the initial placement of the catheter is done under fluoroscopic guidance, the localization during the ablation procedure relies on so-called mapping systems. Although commercial mapping systems have shown reliability in a clinical setting, they do not seem feasible in an experimental setting. Commercial systems often use magnetic- or impedance-based technologies to locate ablation catheters. Magnetic-based approaches use an AC magnetic field generator and pickup coils in the catheter to estimate the pose of the catheter [20]. Impedance-based approaches generate voltage gradients between surface electrodes, which are placed on the patient's body, to reconstruct the catheter pose [20], [21]. However, these systems would require a complex experimental setup as well as expensive tracking equipment.

Furthermore, commercial systems usually do not offer an API to access the location data in real-time. For this reason, we suggest an easy, low-cost setup based on stereo vision to localize the catheter in real-time.

Our setup consists of two UEC-3570 (Somikon, Buggingen, BW, Germany) endoscopic cameras, which are placed in the intended mounts of the anatomical model, as shown in Figs. 1 (A) and (B). The calibrated setup triangulates the 3D position of markers, which are placed on the catheter. We can then estimate the position and orientation of the catheter tip using the geometry of the catheter and the arrangement of the markers.

Before we can triangulate 3D positions from the two camera images, we need to calibrate the cameras intrinsically and extrinsically. Therefore, we first place the cameras in the intended mounts and detach the pulmonary veins from the model. We then move a checkerboard of known geometry behind the left atrium and capture it with both cameras in several different poses. The Matlab Computer Vision Toolbox™ (MathWorks Inc., Natick, MA, USA) allows us to easily derive the calibration matrices and distortion coefficients for each camera from these images [22], [23]. This setup only allows us to determine the 3D localization of a marker in the camera frame $\{c\}$ as shown in Fig. 2 (A). However, we still require the positions in the model frame $\{m\}$.

To obtain the catheter tip pose in $\{m\}$, the transformation T_{mc} between $\{c\}$ and $\{m\}$ must be determined. This is achieved using an AprilTag [24] held on a mount attached to the anatomical model as shown in Figs. 2 (A) and (B). From the geometry of the model, we know the transformation T_{ma} from the AprilTag frame $\{a\}$ to $\{m\}$. We use the AprilTag detection algorithm [24] to determine the static transformation T_{ac}. Subsequently, T_{mc} can be determined by multiplying T_{ma} and T_{ac}.

Ablation catheters usually consist of a rigid tip and a flexible body. Hence, the position and orientation of the catheter tip can be determined based on the 3D positions of the distal and proximal end of the catheter tip. In this setup, green and red color markers are attached to the catheter tip as shown in Fig. 2 (C). To determine the location of a marker in the camera images, we first transform the captured images from the RGB to the HSV color model. We then binarize the images using thresholding for which we determined suitable thresholds experimentally. The center of a marker in a binarized image is then determined using OpenCV [25] and the algorithm presented in [26].

The triangulation of the 3D position of a marker from the two positions in the images is then performed using Direct Linear Transform [27]. We facilitate OpenCV's [25] implementation of this algorithm in our setup. The 3D positions of each marker in the camera frame, ${}^{c}P_g$ and ${}^{c}P_r$, can be determined using this method and can then be transformed to their corresponding positions in the model frame, ${}^{m}P_g$ and ${}^{m}P_r$, using T_{cm}.

The position of the catheter tip P_{tip} is estimated based on the geometry of the catheter and the arrangement of the markers as shown in Fig. 2 (C). As the catheter tip is a rigid body, we can estimate the tip position using

$$P_{tip} = P_r + \frac{1}{2} l_r (\overline{P_g P_r}) \tag{1}$$

with l_r the length of the red marker along the catheter's longitudinal axis. The orientation of the tip $\boldsymbol{v}_{tip}$ is defined by

$$\boldsymbol{v}_{tip} = \frac{\overline{P_g P_r}}{||\overline{P_g P_r}||_2} \tag{2}$$

The tracking system is integrated into a Robot Operating System (ROS)-based application and publishes P_{tip} and $\boldsymbol{v}_{tip}$, which are then used for visualization and evaluation of an experiment [28].

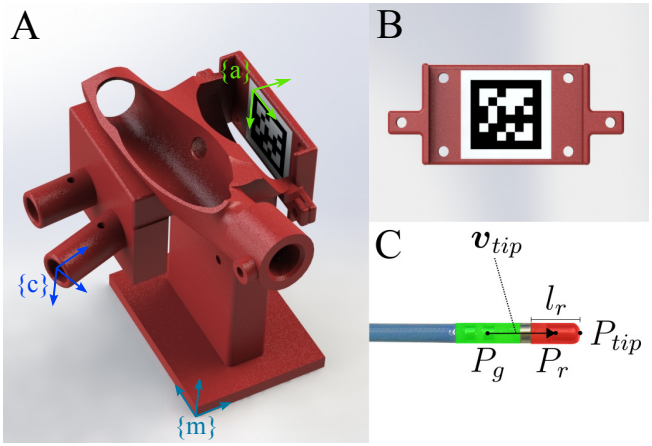

Fig. 2. Calibration and registration of the simulation setup. (A) The reference frames of the model, the camera setup and the AprilTag are indicated by $\{m\}$, $\{c\}$ and $\{a\}$ respectively. Before an experiment is started the camera positions with respect to the anatomical model are calibrated with an AprilTag. The pulmonary vein section of the model is detached and a so-called registration unit (B) is attached in its place to achieve this. (C) After successful calibration of the stereo camera system, the catheter tip position and orientation can then be estimated. Each camera tracks the two color markers and their corresponding 3D positions are then triangulated. Subsequently, the tip position is estimated based on the catheter geometry and the marker arrangement.

C. GUI

Due to the minimally-invasive nature of catheter ablation, the operating surgeon does not have direct visibility of the catheter while steering. The catheter is tracked using a tracking system and displayed on a screen along with the anatomy and the ablation targets. Our platform offers an RViz-based GUI to simulate this scenario as shown in Fig. 3. It allows the user to navigate the catheter based only on feedback displayed on a screen. The GUI guides the user by displaying the ablation targets and helps him to get a sufficient spatial understanding of the current situation.

The GUI displays three main parts: the anatomical model, the real-time catheter tip pose and the ablation targets. The anatomical model is loaded as an STL file and the catheter tip information is obtained from the tracking system. To determine the ablation targets, the GUI allows the user to define the approximate contour around the pulmonary veins.

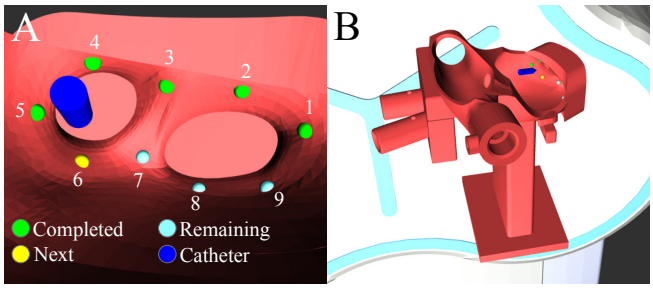

Fig. 3. Graphical user interface for in-vitro pulmonary vein isolation. It displays the ablation targets along with their status. Furthermore, the position and orientation of the catheter tip is indicated by a marker. (A) The selected view perspective makes it easy for the user to see all ablation targets and to monitor the progress of the procedure. The numbers indicate the order of the ablation targets. (B) The user can freely adjust the perspective to get a sufficient spatial understanding of the current situation.

Before an experiment is started, the user can define the desired spacing between two consecutive ablation targets. The GUI then computes the equally-spaced ablation targets on the defined ablation contour using the defined spacing. These ablation targets are then displayed in the GUI along with their state as shown in Fig. 3. A marker can have three different states: *Completed*, *Next* or *Remaining*. This allows the users to track the progress of their experiments. Furthermore, the users can adjust the view perspective to obtain a more holistic spatial understanding as shown in Fig. 3 (B).

D. KPIs

As catheter navigation plays a crucial role in the overall outcome of an ablation procedure, we introduce performance indicators in this section that can be easily assessed with our proposed platform.

1) Procedure duration: The procedure duration is an obvious indicator to evaluate the performance of a surgical system - the shorter the duration of a procedure the higher the number of patients that can be treated daily in a clinic. The procedure duration d is simply defined as $(t_{end} - t_0)$ with t_0 and t_{end} the start time and the end time, respectively.

2) Contact stability: During the delivery of the RF energy, the surgeon must stabilize the catheter at the ablation target as much as possible to make the ablation predictable. This property is assessed with our system by computing the standard deviation of the catheter's position $\sigma_{P_{tip}}$ during the simulated energy delivery at each ablation target.

3) Ablation angle: The ablation angle affects the lesion size and, therefore, the outcome of an ablation [8], [9]. The angle θ between the surface at the ablation target and the catheter tip is then computed as

$$\theta = \pi - \arccos \frac{\boldsymbol{v}_{tip} \cdot (-\boldsymbol{n}_m)}{||\boldsymbol{v}_{tip}||_2 \, ||\boldsymbol{n}_m||_2} \tag{3}$$

with $\boldsymbol{n}_m$ the normal vector of the model surface at the ablation target, which is determined using Version 2.37.13 of Trimesh (2019).

4) Trajectory accuracy: To properly evaluate the navigation performance of an automated system, we propose to assess the catheter's ability to follow a predefined trajectory $P^*_{tip}(t)$ defined or uploaded through our GUI. The catheter's navigation performance $\epsilon_{P_{tip}}$ is defined by the mean distance of the catheter tip to the desired trajectory and can be computed as

$$\epsilon_{P_{tip}} = \frac{1}{T} \sum_{t=0}^{T} ||P^*_{tip}(t) - P_{tip}(t)||_2 \tag{4}$$

with t the index of a time step and T the number of all time steps.

5) User satisfaction: In addition to the system's technical performance, the user satisfaction is assessed by having the user perform several experiments with a system and asking him to rate various aspects of the system using the Likert scale. This could include but is not limited to aspects such as physical exertion, navigation intuitiveness or navigation constraints. We believe this provides an important metric regarding the usability of the system - an important aspect for the surgeon who often performs several procedures in a single day and uses an ablation system for several hours.

III. RESULTS

To demonstrate the usefulness of our evaluation setup, we compare two different navigation approaches: manual navigation and remote magnetic navigation. Before the start of the study, we calibrated the stereo camera setup with 44 checkerboard images resulting in a mean reprojection error of 0.29 pixel. This proof-of-concept study was performed with one user, an engineer with prior experience with both systems, who conducted ten simulated ablation procedures with each navigation system. He started the study with ten consecutive experiments using the manual navigation system and then repeated the process with the magnetic navigation system. For each experiment, we use identical ablation targets with a spacing of 9 mm leading to a total of 9 ablation targets as indicated in Fig. 3. The user was instructed to navigate the catheter to each ablation point in the order indicated by the GUI. An ablation target was considered to be reached if the catheter tip position was within 1.5 mm of the ablation target for 5 consecutive seconds. For the manual navigation, we used the Thermocool SF Nav (Biosense Webster Inc., Irvine, CA, USA). The manual catheter could be navigated by bi-directional bending of the catheter tip and translation and rotation of the catheter base. In the remote magnetic navigation approach, we used the MagnoFlush G4 (MedFact engineering GmbH, Loerrach, BW, Germany). The catheter was then steered using the Navion, an in-house magnetic navigation system, which allowed the user to generate precise external magnetic fields.

A. Procedure Duration

The presented platform allows the user to evaluate the procedure times between different systems. Table I summarises the results of our proof-of-concept study. It shows that the mean procedure times μ_d for manual and magnetic

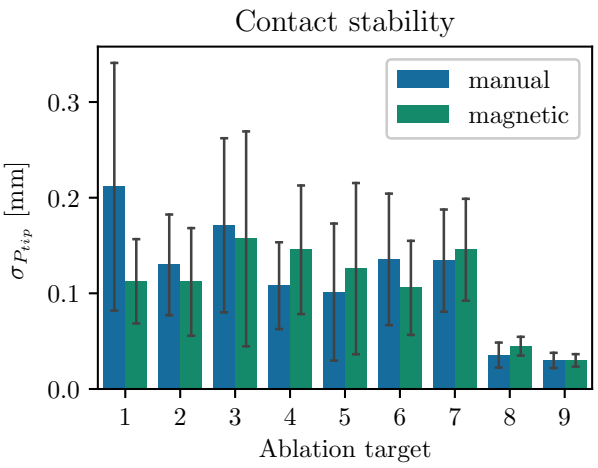

Fig. 4. Standard deviation of the catheter tip position, $\sigma_{P_{tip}}$, during an ablation at different ablation targets. Each bar contains data from ten experiments. The black bars indicate the standard deviation of $\sigma_{P_{tip}}$ at the respective ablation target throughout all experiments.

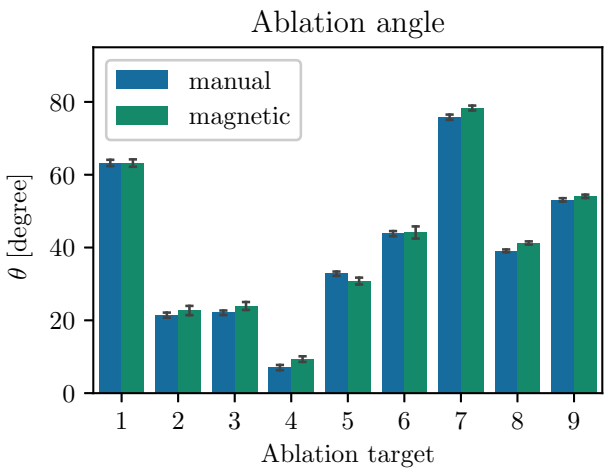

Fig. 5. Ablation angle θ between the catheter tip and the surface at different ablation targets. 0° indicates a parallel ablation and 90° an ablation perpendicular to the surface. Each bar contains data from ten experiments. The black bars indicate the standard deviation of θ at the respective ablation target throughout all experiments.

navigation were 117.4 s and 158.2 s, respectively. Overall, the shortest procedure time was 93.0 s and was observed with manual navigation.

B. Contact Stability

Both systems offered comparable contact stability for most ablation targets as shown in Fig. 4. One observation to note is the contact stability at ablation target 1. During the manual catheter navigation, the user had to apply a high bending force as well as a high torque at the catheter base to reach the target. Since it was strenuous to do both at the same time, the user struggled to hold the catheter at a steady position during the ablation. This was not observed during remote magnetic navigation, showing the potential to outperform manual catheter navigation for difficult to reach ablation targets.

C. Ablation Angle

The ablations angles are depicted in Fig. 5. These were consistent throughout all experiments and between the two systems. The user noticed that neither system allowed for the adjustment of the ablation angle and that the targets could only be reached at specific angles. One interesting observation is that some ablation targets were reached almost perpendicularly (e.g. ablation target 7) while some targets could only be reached almost parallel to the surface (e.g. ablation target 4). Hence, one would expect different lesion sizes for each ablation target [8], [9]. Variable stiffness catheters could be an interesting approach to tackle this problem in the future [29]–[31].

TABLE I

STATISTICS OF PROCEDURE DURATION FOR TWO DIFFERENT NAVIGATION SYSTEMS.

System	μ_d [s]	σ_d [s]	min_d [s]	max_d [s]	# exp
Manual	117.4	11.7	93.0	134.7	10
Magnetic	158.2	54.9	116.7	283.4	10

D. User Satisfaction

Table II shows potential questions along with the user's answers regarding the user satisfaction. The user was asked to rate each of these aspects on a scale from 1 (strongly disagree) to 5 (strongly agree). The user reported more intuitive steering using the manual navigation system. The steering of the magnetic navigation system resulted in less physical exertion. This kind of user feedback gives valuable starting points for further system improvements.

IV. CONCLUSION

In this paper, we presented a platform to simulate pulmonary vein isolation and to evaluate the performance of navigation systems for catheter ablation. An anatomical model containing the relevant heart structures was 3D printed. This model contained mounts for two endoscopic cameras, which were used for the 3D localization of the ablation catheter. The catheter tip is equipped with two color markers that are tracked by each of the cameras. After the calibration of the stereo camera setup, the 3D positions of the markers can be triangulated and the catheter tip pose is estimated. We introduced a GUI in which the information about the catheter tip, the ablation targets and the anatomy is combined in a common reference frame. This allowed the user to navigate an ablation catheter based on visual feedback from the GUI similar to a real scenario. This setup allowed the user to analyze various performance metrics that are collected throughout the simulated pulmonary vein isolation. Furthermore, we demonstrated the usefulness of the presented setup and KPIs in a proof-of-concept study.

TABLE II

POTENTIAL QUESTIONS TO ASSESS THE USER SATISFACTION OF A CATHETER ABLATION SYSTEM.

	Manual					Magnetic				
Question	1	2	3	4	5	1	2	3	4	5
1. I found it intuitive to steer the catheter in a desired direction.	☐	☐	☐	☐	☒	☐	☐	☒	☐	☐
2. I found it physically exhausting to perform several experiments in a row.	☐	☐	☐	☒	☐	☒	☐	☐	☐	☐
3. I had to operate the system at its limits to reach all ablation targets.	☐	☐	☐	☒	☐	☐	☐	☒	☐	☐

The main limitations of our evaluation platform are the absence of blood flow and heart contraction. Despite these limitations, we are convinced that the presented setup offers a reliable way to assess the navigation properties of ablation systems in the context of an in-vitro study. In the future, we plan to use this platform to assess the performance of different magnetic navigation approaches in the scope of representative user studies. In particular, we are working towards the automation of the navigation to allow surgeons to perform catheter ablation procedures in a more efficient and reproducible manner. This is of particular interest in the upcoming years considering the ongoing rise of atrial fibrillation cases. Furthermore, we are investigating teleoperation approaches to conduct catheter ablation procedures remotely from anywhere. This will help to tackle the lack of trained personnel in rural areas and allow experts from around the world to bring their expertise to these areas.

ACKNOWLEDGMENT

This paper is supported by European Union's Horizon 2020 research and innovation programme under grant agreement No 101016834, project HosmartAI (Hospital Smart development based on AI) and by SNSF's BRIDGE progamme under the grant agreement No 180861.

SUPPLEMENTARY MATERIAL

The supplementary material can be found in ETH Zurich's Research Collection (https://www.research-collection.ethz.ch/handle/20.500.11850/584391).

This material includes the STL files of the main part, the ablation section and the registration unit. It also includes a CSV file containing the coordinates of the ablation trajectory from the proof-of-concept study. All models and coordinates are given in $\{m\}$.

REFERENCES

[1] E. J. Benjamin, P. Muntner, A. Alonso, M. S. Bittencourt, C. W. Callaway, A. P. Carson, A. M. Chamberlain, A. R. Chang, S. Cheng, S. R. Das, F. N. Delling, L. Djousse, M. S. Elkind, J. F. Ferguson, M. Fornage, L. C. Jordan, S. S. Khan, B. M. Kissela, K. L. Knutson, T. W. Kwan, D. T. Lackland, T. T. Lewis, J. H. Lichtman, C. T. Longenecker, M. S. Loop, P. L. Lutsey, S. S. Martin, K. Matsushita, A. E. Moran, M. E. Mussolino, M. O'Flaherty, A. Pandey, A. M. Perak, W. D. Rosamond, G. A. Roth, U. K. Sampson, G. M. Satou, E. B. Schroeder, S. H. Shah, N. L. Spartano, A. Stokes, D. L. Tirschwell, C. W. Tsao, M. P. Turakhia, L. B. VanWagner, J. T. Wilkins, S. S. Wong, S. S. Virani, and null null, "Heart disease and stroke statistics—2019 update: A report from the american heart association," *Circulation*, vol. 139, no. 10, pp. e56–e528, 2019.

[2] S. Colilla, A. Crow, W. Petkun, D. E. Singer, T. Simon, and X. Liu, "Estimates of current and future incidence and prevalence of atrial fibrillation in the u.s. adult population," *The American Journal of Cardiology*, vol. 112, pp. 1142–1147, Oct. 2013.

[3] I. Savelieva and J. Camm, "Update on atrial fibrillation: Part i," *Clinical Cardiology*, vol. 31, no. 2, pp. 55–62, 2008.

[4] B. P. Krijthe, A. Kunst, E. J. Benjamin, G. Y. H. Lip, O. H. Franco, A. Hofman, J. C. M. Witteman, B. H. Stricker, and J. Heeringa, "Projections on the number of individuals with atrial fibrillation in the european union, from 2000 to 2060," *European Heart Journal*, vol. 34, pp. 2746–2751, July 2013.

[5] U. Schotten, S. Verheule, P. Kirchhof, and A. Goette, "Pathophysiological mechanisms of atrial fibrillation: A translational appraisal," *Physiological Reviews*, vol. 91, pp. 265–325, Jan. 2011.

[6] H. Essa, A. M. Hill, and G. Y. Lip, "Atrial fibrillation and stroke," *Cardiac Electrophysiology Clinics*, vol. 13, pp. 243–255, Mar. 2021.

[7] E. N. Prystowsky, B. J. Padanilam, and R. I. Fogel, "Treatment of atrial fibrillation," *JAMA*, vol. 314, p. 278, July 2015.

[8] F. H. Wittkampf and H. Nakagawa, "RF catheter ablation: Lessons on lesions," *Pacing and Clinical Electrophysiology*, vol. 29, pp. 1285–1297, Nov. 2006.

[9] V. Calzolari, L. D. Mattia, F. Basso, M. Crosato, A. Scalon, P. A. M. Squasi, S. D. Favero, and C. Cernetti, "Ablation catheter orientation: In vitro effects on lesion size and in vivo analysis during PVI for atrial fibrillation," *Pacing and Clinical Electrophysiology*, vol. 43, pp. 1554–1563, Nov. 2020.

[10] A. Bhaskaran, M. A. Barry, S. I. A. Raisi, W. Chik, D. T. Nguyen, J. Pouliopoulos, C. Nalliah, R. Hendricks, S. Thomas, A. L. McEwan, P. Kovoor, and A. Thiagalingam, "Magnetic guidance versus manual control: comparison of radiofrequency lesion dimensions and evaluation of the effect of heart wall motion in a myocardial phantom," *Journal of Interventional Cardiac Electrophysiology*, vol. 44, pp. 1–8, June 2015.

[11] G. Wu, Q. Luo, Y. Bao, Y. Wei, C. Lin, N. Zhang, T. Ling, K. Chen, W. Pan, L. Wu, Y. Xie, and Q. Jin, "The feasibility of using remote magnetic navigation system as the primary technological training tool for novice cardiac electrophysiology operators in the catheter ablation of left-sided accessory pathway," *Cardiology Journal*, Mar. 2022.

[12] M. P. Armacost, J. Adair, T. Munger, R. R. Viswanathan, F. M. Creighton, D. T. Curd, and R. Sehra, "Accurate and reproducible target navigation with the stereotaxis niobe® magnetic navigation system," *Journal of Cardiovascular Electrophysiology*, vol. 18, pp. S26–S31, Dec. 2006.

[13] D. Steven, T. Rostock, H. Servatius, B. Hoffmann, I. Drewitz, K. Müllerleile, T. Meinertz, and S. Willems, "Robotic versus conventional ablation for common-type atrial flutter: A prospective randomized trial to evaluate the effectiveness of remote catheter navigation," *Heart Rhythm*, vol. 5, pp. 1556–1560, Nov. 2008.

[14] C. Pappone, G. Vicedomini, F. Manguso, F. Gugliotta, P. Mazzone, S. Gulletta, N. Sora, S. Sala, A. Marzi, G. Augello, L. Livolsi, A. Santagostino, and V. Santinelli, "Robotic magnetic navigation for atrial fibrillation ablation," *Journal of the American College of Cardiology*, vol. 47, pp. 1390–1400, Apr. 2006.

[15] W. Saliba, V. Y. Reddy, O. Wazni, J. E. Cummings, J. D. Burkhardt, M. Haissaguerre, J. Kautzner, P. Peichl, P. Neuzil, V. Schibgilla, G. Noelker, J. Brachmann, L. D. Biase, C. Barrett, P. Jais, and A. Natale, "Atrial fibrillation ablation using a robotic catheter remote control system," *Journal of the American College of Cardiology*, vol. 51, pp. 2407–2411, June 2008.

[16] K. R. J. Chun, B. Schmidt, B. Köktürk, R. Tilz, A. Fürnkranz, M. Konstantinidou, E. Wissner, A. Metzner, F. Ouyang, and K.-H. Kuck, "Catheter ablation – new developments in robotics," *Herz Kardiovaskuläre Erkrankungen*, vol. 33, pp. 586–589, Dec. 2008.

[17] L. D. Biase, Y. Wang, R. Horton, G. J. Gallinghouse, P. Mohanty, J. Sanchez, D. Patel, M. Dare, R. Canby, L. D. Price, J. D. Zagrodzky, S. Bailey, J. D. Burkhardt, and A. Natale, "Ablation of atrial fibrillation utilizing robotic catheter navigation in comparison

to manual navigation and ablation: Single-center experience," *Journal of Cardiovascular Electrophysiology*, vol. 20, pp. 1328–1335, Dec. 2009.

[18] Q. Boehler, C. Chautems, L. Sabbatini, F. Duru, and B. Nelson, "A system for in vitro evaluation of magnetic and manual catheter navigation for cardiac ablations," in *Proceedings, Hamlyn Symposium on Medical Robotics 2018*, pp. 3–4, The Hamlyn Centre, Imperial College London, 2018.

[19] S. A. Jones, M. Yamamoto, J. O. Tellez, R. Billeter, M. R. Boyett, H. Honjo, and M. K. Lancaster, "Distinguishing properties of cells from the myocardial sleeves of the pulmonary veins," *Circulation: Arrhythmia and Electrophysiology*, vol. 1, pp. 39–48, Apr. 2008.

[20] V. Y. Reddy, "60 - mapping and imaging," in *Cardiac Electrophysiology: From Cell to Bedside (Sixth Edition)* (D. P. Zipes and J. Jalife, eds.), pp. 581–593, Philadelphia: W.B. Saunders, sixth edition ed., 2014.

[21] Y. Jiang, D. Farina, M. Bar-Tal, and O. Dossel, "An impedance-based catheter positioning system for cardiac mapping and navigation," *IEEE Transactions on Biomedical Engineering*, vol. 56, pp. 1963–1970, Aug. 2009.

[22] J. Heikkila and O. Silven, "A four-step camera calibration procedure with implicit image correction," in *Proceedings of IEEE Computer Society Conference on Computer Vision and Pattern Recognition*, pp. 1106–1112, 1997.

[23] Z. Zhang, "A flexible new technique for camera calibration," *IEEE Transactions on Pattern Analysis and Machine Intelligence*, vol. 22, no. 11, pp. 1330–1334, 2000.

[24] J. Wang and E. Olson, "AprilTag 2: Efficient and robust fiducial detection," in *2016 IEEE/RSJ International Conference on Intelligent Robots and Systems (IROS)*, pp. 4193–4198, IEEE, oct 2016.

[25] G. Bradski, "The OpenCV Library," *Dr. Dobb's Journal of Software Tools*, 2000.

[26] S. Suzuki and K. be, "Topological structural analysis of digitized binary images by border following," *Computer Vision, Graphics, and Image Processing*, vol. 30, pp. 32–46, Apr. 1985.

[27] R. Hartley and A. Zisserman, *Multiple View Geometry in Computer Vision*. Cambridge University Press, Mar. 2004.

[28] M. Quigley, K. Conley, B. Gerkey, J. Faust, T. Foote, J. Leibs, R. Wheeler, A. Y. Ng, *et al.*, "Ros: an open-source robot operating system," in *ICRA workshop on open source software*, vol. 3, p. 5, Kobe, Japan, 2009.

[29] Y. Piskarev, J. Shintake, C. Chautems, J. Lussi, Q. Boehler, B. J. Nelson, and D. Floreano, "A variable stiffness magnetic catheter made of a conductive phase-change polymer for minimally invasive surgery," *Advanced Functional Materials*, p. 2107662, Feb. 2022.

[30] C. Chautems, A. Tonazzini, Q. Boehler, S. H. Jeong, D. Floreano, and B. J. Nelson, "Magnetic continuum device with variable stiffness for minimally invasive surgery," *Advanced Intelligent Systems*, vol. 2, p. 1900086, Oct. 2019.

[31] C. Chautems, A. Tonazzini, D. Floreano, and B. J. Nelson, "A variable stiffness catheter controlled with an external magnetic field," in *2017 IEEE/RSJ International Conference on Intelligent Robots and Systems (IROS)*, IEEE, Sept. 2017.